Chinese Chemical Letters 36 (2025) 110105

Contents lists available at ScienceDirect

Chinese Chemical Letters

journal homepage: www.elsevier.com/locate/cclet

Ultra-high signal-to-noise ratio near-infrared chemiluminescent probe for *in vivo* sensing singlet oxygen

Meiling Zhao[1], Yao Lu[1], Yutao Zhang*, Haoyun Xue, Zhiqian Guo*

State Key Laboratory of Bioreactor Engineering, Key Laboratory for Advanced Materials and Institute of Fine Chemicals, Joint International Research Laboratory of Precision Chemistry and Molecular Engineering, Feringa Nobel Prize Scientist Joint Research Center, Frontiers Science Center for Materiobiology and Dynamic Chemistry, School of Chemistry and Molecular Engineering, East China University of Science and Technology, Shanghai 200237, China

ARTICLE INFO

Article history:
Received 29 April 2024
Revised 7 June 2024
Accepted 11 June 2024
Available online 14 June 2024

Keywords:
Fluorescent probe
Near-infrared
Chemiluminescent
Singlet oxygen
Bioimaging

ABSTRACT

Singlet oxygen ($^1O_2$), as the primary reactive oxygen species in photodynamic therapy, can effectively induce excessive oxidative stress to ablate tumors and kill germs in clinical treatment. However, monitoring endogenous $^1O_2$ is greatly challenging due to its extremely short lifetime and high reactivity in biological condition. Herein, we report an ultra-high signal-to-ratio near-infrared chemiluminescent probe (DCM-Cy) for the precise detection of endogenous $^1O_2$ during photodynamic therapy (PDT). The methoxy moiety was removed from enolether unit in DCM-Cy to suppress the potential self-photooxidation reaction, thus greatly eliminating the photoinduced background signals during PDT. Additionally, the compact cyclobutane modification of DCM-Cy resulted in a significant 6-fold increase in cell permeability compared to conventional adamantane-dioxane probes. Therefore, our "step-by-step" strategy for DCM-Cy addressed the limitations of traditional chemiluminescent (CL) probes for $^1O_2$, enabling effectively tracking of endogenous $^1O_2$ level changes in living cells, pathogenic bacteria and mice in PDT.

Singlet oxygen ($^1O_2$), the lowest excited electronic state of molecular oxygen, exhibits significantly enhanced reactivity in comparison to oxygen in its triplet ground state [1-3]. In clinical photodynamic therapy (PDT), this heightened reactivity of $^1O_2$ facilitates the oxidation of nearby biomolecules, triggering inflammatory responses or immune reactions, ultimately resulting in tumor ablation or bacteria eradication [4-10]. Hence, real-time visualization of $^1O_2$ in living cells and pathological tissue is of paramount importance to elucidate its mechanism of action in medical processes and optimize therapy protocols [11-15]. Currently, the gold standard for $^1O_2$ determination is the measurement of the phosphorescence of $^1O_2$ at 1270 nm [16,17]. However, the short luminescence lifetime and extremely low quantum yield of $^1O_2$ lead to weak phosphorescence, severely limiting its biological application. Reaction-based optical probes offer an alternative strategy for $^1O_2$ detection under biological condition due to their high sensitivity and non-invasive features [18-20]. Particularly, chemiluminescent probes, which emit light through specific chemical reactions with $^1O_2$, does not require real-time excitation light irradiation, effectively eliminating interference from light scattering and autofluorescence with fluorescent probes. This characteristic enables unprecedented sensitivity and selectivity [21-24].

Despite the significant advantages of chemiluminescence for biomarker sensing, the development of chemiluminescent probes is still in its infancy, with merely a few cases enabling imaging $^1O_2$ in living cells and animals [25,26]. In general, several factors including photo-induced self-oxidation during photodynamic therapy (PDT), poor cell permeability, and short emission wavelengths greatly limit the *in vivo* application of the $^1O_2$ imaging probes: (i) Photo-induced self-oxidation: our previous work revealed that chemiluminescent precursors containing electron-rich enolether unit are prone to undergo photo-oxidation reaction accompanied by chemiluminescence generation, potentially leading to an overestimation of singlet oxygen [27]; (ii) Poor cell permeability: despite efforts to enhance stability of dioxane through the incorporation of adamantane units, the rigidity and increased steric hindrance reduce the cell membrane permeability of Schaap's dioxetane. This limitation has necessitated modifications such as the incorporation of membrane-penetrating peptides like polyarginine to enhance the cell permeability of the probes [28]; (iii) Short emission wavelengths: conventional chemiluminescent probes for $^1O_2$ sensing emit visible light, which has limited tissue penetration capabilities [29,30]. To the best of our knowledge, current singlet

* Corresponding authors.
E-mail addresses: 1539232010@qq.com (Y. Zhang), guozq@ecust.edu.cn (Z. Guo).
[1] These authors contributed equally to this work.

https://doi.org/10.1016/j.cclet.2024.110105
1001-8417/

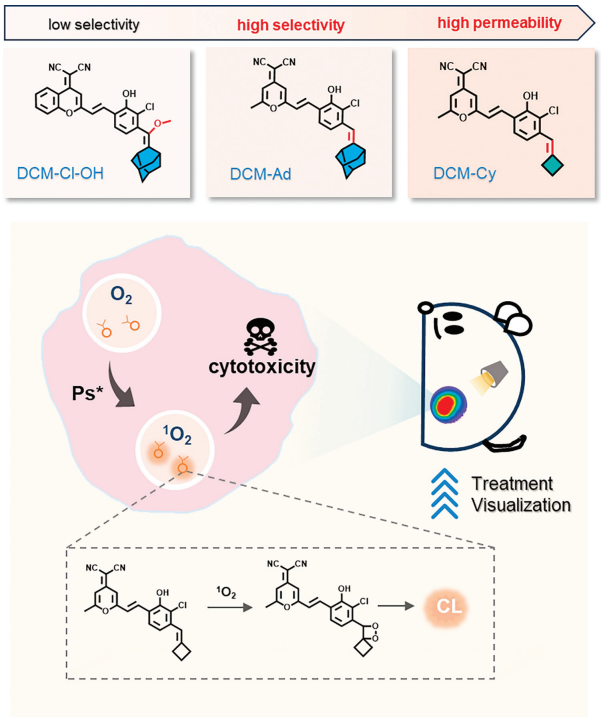

Fig. 1. Schematic illustration of "step-by-step" design strategy for CL probes for ultra-high signal-to-ratio $^1O_2$ detection: (i) removing the methoxy moiety from enolether unit to suppress the potential self-photooxidation reaction; (ii) replacing the rigid and bulky adamantane units with a compact cyclobutane moiety significantly enhanced the cell permeability.

oxygen probes cannot resolve all of these challenges simultaneously. Consequently, the development of a self-photooxidation resistant near-infrared (NIR) chemiluminescent (CL) probe for the *in vivo* $^1O_2$ detection is highly demand.

Herein, we presented two CL probes, DCM-Ad and DCM-Cy, for *in vivo* $^1O_2$ imaging in living cells, viruses, and mice models during PDT. Our "step-by-step" strategy focuses on addressing the inherent limitations of traditional CL probes for $^1O_2$ determination and improving their biological applicability (Fig. 1). We hypothesized that reducing the electron cloud density of enolether unit could effectively mitigate the photo-oxidation of chemiluminescent probes. Thus, compared the conventional CL probes, we removed the methoxy group to minimize the photoinduced background signals during PDT. Subsequently, we replaced the rigid and bulky adamantane units by compact cyclobutane building blocks to improve its cell permeability capabilities. In the presence of $^1O_2$, the probe DCM-Cy undergo oxidation to form an unstable strained phenol-dioxetane intermediate, which rapidly spontaneous decomposes to generate an excited carbonyl species. This species then decays to its ground state, accompanied by the emission of NIR chemiluminescence. DCM-Cy exhibits remarkable resistance to photo-oxidation with minimal background signal interference, with an approximately 6-fold enhancement in cell permeability capabilities. Consequently, based on our step-by-step molecular design strategy, the probe DCM-Cy possesses the capability to monitor *in vivo* levels of $^1O_2$ in bacteria, living cells, and mice during photodynamic therapy.

The general synthesis procedure of DCM-Ad and DCM-Cy are depicted in Scheme S1 (Supporting information). 2-Chloro-3-hydroxybenzaldehyde was chosen to undergo four steps to synthesize key intermediates compounds **1–5** which contains of ethyl phosphonates. In the ^1H NMR spectrum, we observed a characteristic methylene signal ($\delta = 3.39$ ppm, d, $J = 16.0$ Hz), indicative of the proton attached to ethyl phosphonates. Subsequently, reacted with cyclobutanone or adamantanone to form a double bond, through which phenoxy was attached to adamantane or cyclobutene without methyl acrylate. After two synthetic steps, lastly, such structure backbone was finally attached to an acceptor, dicyanomethylchromone in a yield of about 30%. Characteristic protons on adamantane of DCM-Ad ($\delta = 1.84$–2.01 ppm, m, 12H) and cyclobutene of DCM-Cy ($\delta = 2.15$–3.10 ppm, 6H) were found in the ^1H NMR spectrum. The mass spectra of DCM-Ad and DCM-Cy were also confirmed their molecular weight value of 455.1526 and 375.0898, respectively, completely matching with the calculated value 455.1521 and 375.0895. All the key compounds were characterized by ^1H NMR, ^{13}C NMR spectra, and high-resolution mass spectrometry (HRMS).

With these probes in hand, we firstly evaluated their chemiluminescent response ability toward $^1O_2$. The mixed solutions of H_2O_2/NaClO were chosen as the $^1O_2$ donor, and the $^1O_2$ concentration was almost the equivalent to that of NaClO (the conversion efficiency was near 100%). As shown in Fig. 2A, with the presence of 70 equiv. $^1O_2$, the CL signals of DCM-Cy and DCM-Ad exhibited remarkable growth at the primary emission peak around 650 nm, while negligible CL signal was found in the absence of $^1O_2$. To investigate the capability of these probes to sense $^1O_2$, clinically photosensitizer Rose Bengal (RB) was chosen to produce $^1O_2$ upon light irradiation in PDT [31]. In the presence of 10 μmol/L RB, the intensity of DCM-Cy and DCM-Ad increased with the extension of illumination time (LED white light, 96 mW/cm^2) and attained a maximum CL signal at 70 s (Fig. 2B and Fig. S1 in Supporting information). Notably, there was a good linear correlation between the CL intensity of these probes and the concentration of RB, indicating that the $^1O_2$ generated by RB is intuitively detected and quantified by CL signal changes (Fig. S2 in Supporting information). Furthermore, compared to commercially available probe DCFH, DCM-Cy had a higher signal-to-noise ratio for the detection of $^1O_2$ (Fig. S3 in Supporting information). These results indicated that DCM-Cy and DCM-Ad has the capability of ultra-sensitive detection of $^1O_2$ levels in aqueous solutions.

The selectivity of the CL probe is an essential factor and serves as a critical criterion for assessing potential future applications [32,33]. Thus, we assessed the capability of DCM-Cy and DCM-Ad to specifically sense of $^1O_2$ with other biological reactive oxygen species (ROS) [34]. As expected, when treated with $^1O_2$, an remarkable enhancement of CL signals was observed (Fig. 2C). However, there were only negligible increases in CL intensity upon the incubation with other ROS (10 equiv. of H_2O_2, ClO^-, $^{\bullet}OH$, $O_2^{\bullet-}$, $ONOO^-$, respectively). These results demonstrate the excellent selectivity of DCM-Cy and DCM-Ad toward $^1O_2$ over other potential ROS.

Undesirable photo-oxidation reactions are potential contributor to the background noise signal generated by conventional $^1O_2$ detector when exposed to light. Our previous investigations have demonstrated that CL precursors containing electron-rich enolether units are susceptible to self-photooxidation, leading to chemiluminescent emission. In DCM-Cy and DCM-Ad, the methoxy groups were removed from enolether building block to enhance the resistance to self-photooxidation. Comparing with reported DCM-Cl-OH [35], these probes show much low background CL signals under light irradiation (Fig. S4 in Supporting information), suggesting significant improvements in resistance to self-photooxidation.

In a simulated PDT test, both DCM-Ad and DCM-Cy exhibited ultra-high signal-to-noise ratio (the CL signals ratio in the presence and absence of photosensitizer) of $^1O_2$ sensing, with 433- and 466-fold CL signals enhancement, respectively. The distinct change is significantly higher than that of DCM-Cl-OH (Fig. 2D). Moreover, we recorded the CL kinetic profile of DCM-Cy and DCM-Ad, which exhibited a typical glow-type CL behavior: The CL half-time of

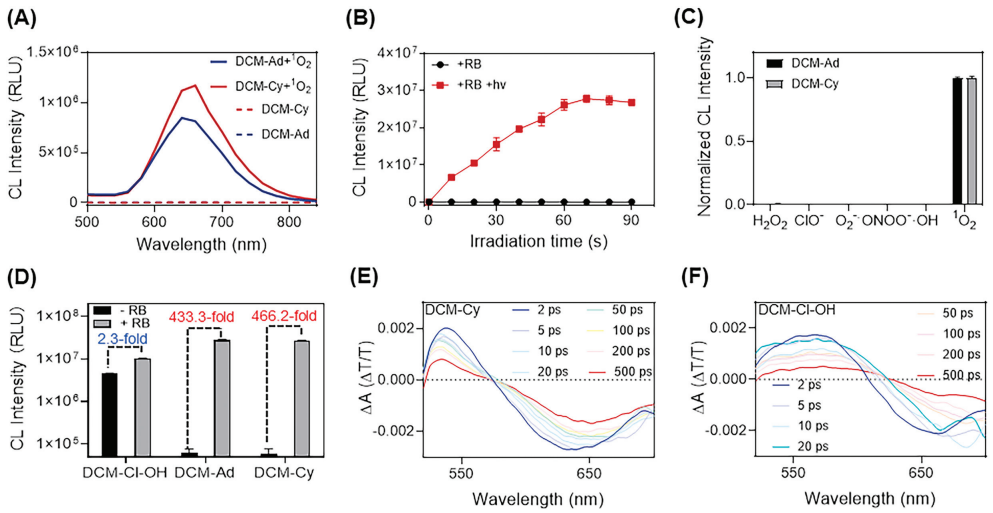

Fig. 2. Chemiluminescent response of DCM-Ad and DCM-Cy towards $^1O_2$. Test condition: Tris–HCl buffer solution, containing 4 mg/mL bovine albumin (BSA), pH 7.5. (A) Chemiluminescence spectrum of probes (20 μmol/L) in the absence or presence of 70 equiv. $^1O_2$ (H_2O_2/NaClO system). (B) Time dependent CL intensity changes of DCM-Cy mixed with equal RB in presence and absence of light irradiation. (C) Selectivity of DCM-Ad and DCM-Cy towards various ROS, $^1O_2$, H_2O_2, ClO^-, $O_2^{\bullet-}$, $ONOO^-$, $^{\bullet}OH$ (100 μmol/L), in aqueous system. (D) The chemiluminescence of DCM-Ad, DCM-Cy and previous CL probes DCM-Cl-OH in the presence or absence of RB under light exposure (10 μmol/L, 96 mW/cm^2 white LED light for 60 s). Femtosecond time-resolved transient absorption spectra of 0.1 mmol/L DCM-Cy (E) and DCM-Cl-OH (F) in Tris–HCl solutions (containing 20 mg/mL BSA) pumped at 500 nm. Data are presented as mean ± standard deviation (SD) ($n = 3$).

DCM-Cy and DCM-Ad was about 38 s and 53 s, respectively (Fig. S5 in Supporting information). Thus, the CL signal from these probes remained to be detectable even within 5 min. The above results indicate that DCM-Cy and DCM-Cy possess a high contrast detection potentiality for $^1O_2$ during clinical photodynamic therapy.

To gain insight into the self-photooxidation resistant ability of DCM-Cy and DCM-Ad for $^1O_2$ detection in PDT, we investigated the photoinert mechanism of these probes by femtosecond transient spectroscopy (fs-TA) [36]. As shown in Fig. 2E, the TA spectra of DCM-Cy show two distinct bands with time-wavelength dependence. The negative excited state absorption (ESA) signals, observed at wavelengths exceeding 630 nm, is attributed to stimulated emission (SE). On the other hand, the band observed at wavelengths below 530 nm is attributed to excited state absorption. In contrast, the TA spectra of our reported DCM-Cl-OH displayed two positive excited state absorption signals peaking at 545 and 575 nm in the water solution (Fig. 2F and Fig. S6 in Supporting information). The excited state species at the 575 nm should potentially play a crucial role in the photooxidation reaction with oxygen, resulting in a high background CL upon light irradiation. The elimination of methoxy groups from the enolether units effectively prevents the formation of similar excited state species in the probes, thereby signally reducing the background signal.

The aforementioned experiments demonstrated the high selectivity, and minimized background signals of DCM-Ad and DCM-Cy, encouraging us to further investigate the ability of these probes for intracellular $^1O_2$. Prior to employing these probes in living cells, it was imperative to validate their biocompatibility. The cytotoxicity of the probes towards HeLa cells was assessed using the methyl thiazolyl tetrazolium (MTT) assay. After incubation with different concentrations of DCM-Ad and DCM-Cy for 24 h, the cell survival rates were estimated to be over 79% and 81%, respectively, indicating their favorable biocompatibility. Additionally, an extra irradiation process (96 mW/cm^2, 5 min) is added after incubation with probes for 2 h to evaluate their phototoxicity. After 24 h of incubation, the cell survival rates were more than 75%, demonstrating the negligible toxicity of the probes exposed under light during PDT (Fig. S7 in Supporting information).

Previous studies have demonstrated that the poor permeability of CL probes is one of the major bottlenecks impeding intracellular probe *in vivo* sensing. Specifically, the rigid and bulky adamantane units are identified as potential factors resulting into poor permeability in these conventional reported CL probes [30,37]. Hence, we suppose that the presence of a compact cyclobutane building block could greatly improve cell permeability of the probes. Subsequently, the confocal microscopy was employed to validate the cell permeability of the DCM-Ad and DCM-Cy. DCM-Ad and DCM-Cy exhibit fluorescent signals in the near-infrared under 500 nm excitation light (Fig. S8 and Table S1 in Supporting information). As shown in Fig. 3A, after incubation with DCM-Cy for 1 min, a distinct NIR fluorescent signal at 650 nm was observed in the HeLa cells, as well as the intracellular fluorescence signal reaching maximum at approximately 4 min. By contrast, DCM-Ad required nearly 25 min to reach the maximum intracellular fluorescence intensity, which is almost six times longer than that of required by DCM-Cy (Fig. 3B). Additionally, the maximum intracellular brightness of DCM-Cy was about 10% higher than that of DCM-Ad, indicating a superior potential for intracellular sensing (Fig. 3C). These results suggest that DCM-Cy not only showed a dramatic enhancement in cell permeability but also an increase in cellular uptake.

Then, we evaluated the intracellular $^1O_2$ sensing capabilities of these probes during photodynamic therapy. Given its excellent cell permeability and cellular uptake capability, DCM-Cy was chosen for *in vitro* biological testing. HeLa cells were incubated with DCM-Cy and RB for 2 h. Subsequently, these cells were irradiated by white LED light for 3 min and then their chemiluminescence signals was captured by ImageQuant LAS4000 system. As shown in Fig. 4A, the cells that incubated with DCM-Cy and RB, followed by light irradiation, exhibited a pronounced CL signals. Conversely, cells that were merely incubated with DCM-Cy (lacking $^1O_2$ donor) or RB (lacking $^1O_2$ probe), did not produce any detectable chemiluminescence signal upon light irradiation. Furthermore, cells that were maintained in a dark environment did not exhibit any chemiluminescence signals (Fig. 4B).

Eradicating pathogenic bacteria or inhibiting bacterial proliferation represents a crucial aspect of photodynamic therapy [38-43]. Hence, we further explored the capacity of these probes to detect the endogenous $^1O_2$ in bacteria. Initially, we investigated the bacterial internalization capabilities of these probes using fluorescence confocal microscopy. As shown in Fig. 4C, remarkable flu-

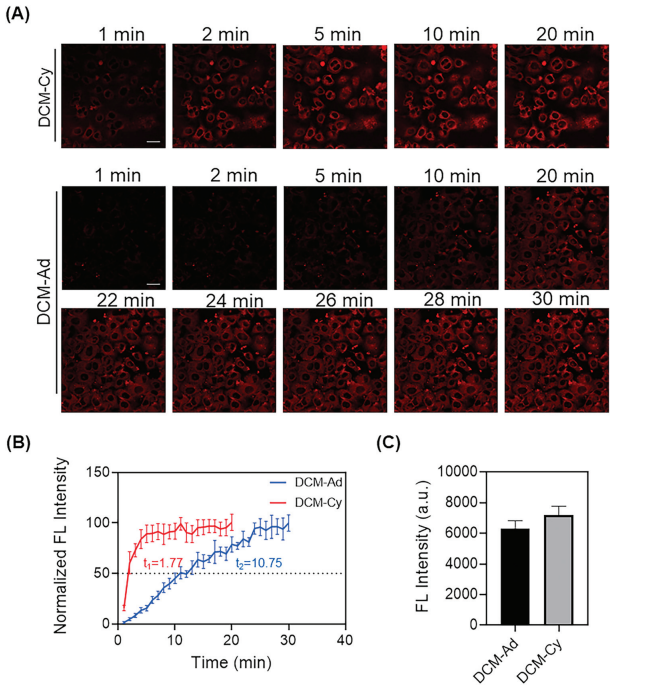

Fig. 3. Confocal Microscopy imaging the cellular internalization of DCM-Cy and DCM-Ad. (A) Fluorescence imaging of DCM-Cy and DCM-Ad in HeLa cells over time. Scale bar: 30 μm. (B) Quantification of intracellular fluorescence signals with different incubation times. (C) Comparison of intracellular fluorescence intensity of DCM-Ad and DCM-Cy at equilibrium state. Error bars represent standard deviations ($n = 6$).

orescent signals were observed in *Staphylococcus aureus* following incubation with DCM-Ad or DCM-Cy, indicating efficient uptake of the probes by the bacteria. Subsequently, we tested whether these probes can detect $^1O_2$ produced in bacteria during the PDT process. Upon exposure to LED light, bright chemiluminescence signals were detected in *Staphylococcus aureus* following co-incubation with DCM-Cy and RB for 1 h (Fig. 4D), in which the chemiluminescent intensity was approximately 10-fold higher than that of the control group without light irradiation. These results provide solid evidence for the ability of DCM-Cy to detect endogenous $^1O_2$ in living cells and pathogenic bacteria produced during the PDT process.

Encouraged by the excellent capacity of DCM-Cy to image intercellular $^1O_2$, we expect utilization DCM-Cy to image $^1O_2$ production during PDT *in vivo*. All animal experiments were performed according to the guidelines of the Care and Use of Laboratory Animals formulated by the Ministry of Science and Technology of China and were approved by the Animal Care and Use Committee of East China University of Science and Technology (2021–07,001). The nude mice bearing HeLa xenograft tumor were selected as *in-vivo* animal models. After Intratumoral injection of the DCM-Cy or a mixture of DCM-Cy and RB for 30 min, and subsequent exposure to white light for 1 min, the chemiluminescence signals were immediately acquired by an IVIS living imaging system. As shown in Fig. 5A, the conventional chemiluminescent probe, DCM-Cl-OH, exhibited a noticeable background signal caused by self-photooxidation even in the absence of the photosensitizer. Upon the addition of the photosensitizer, the chemiluminescence signal was merely enhanced 4.4-fold. In contrast, the DCM-Cy group displayed minimal background signals in the absence of the photosensitizer, which is consistent with solution test results (Fig. 5B). Consequently, a remarkable 95-fold increase in signal-to-noise ratio was achieved following the introduction of the photosensitizer. Collectively, all these tests indicate that DCM-Cy can be fully ap-

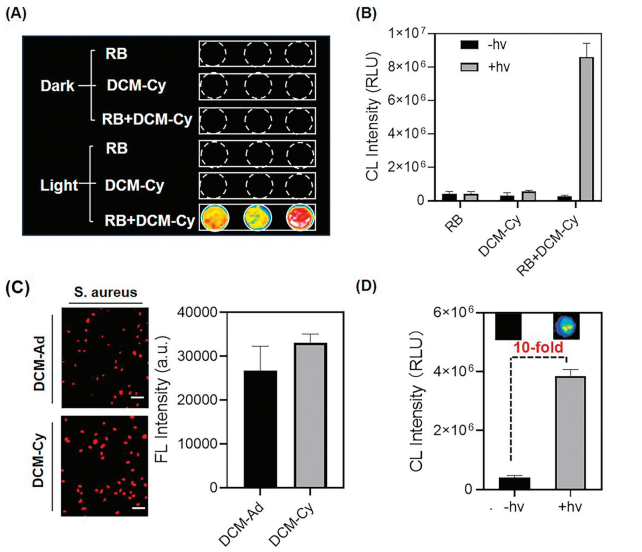

Fig. 4. Monitoring of endogenous $^1O_2$ in HeLa cells and *Staphylococcus aureus*. (A) Chemiluminescence images acquired in HeLa cells after incubation with RB, DCM-Cy (10 μmol/L) alone, or simultaneously for 2 h upon exposure to LED light or in darkness. (B) Quantification of the CL intensity in figure A. (C) Confocal fluorescence imaging of DCM-Ad and DCM-Cy in *Staphylococcus aureus* and the quantitative fluorescence intensity. Scale bar: 30 μm. (D) *Staphylococcus aureus* was co-incubated with DCM-Cy and RB for 1 h, and then the chemiluminescence intensity was measured with or without white LED light irradiation. Insert: CL imaging of DCM-Cy in *Staphylococcus aureus*. Error bars represent standard deviations ($n = 3$).

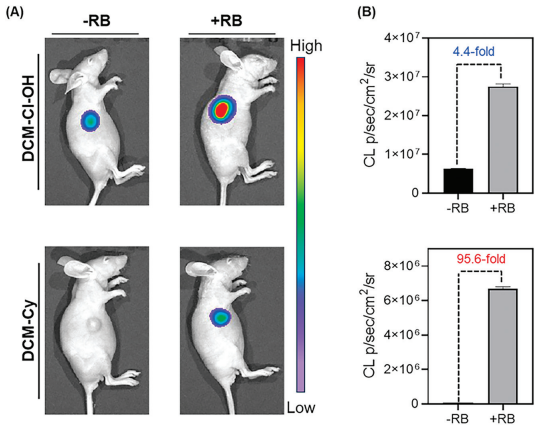

Fig. 5. *In vivo* imaging of intratumor $^1O_2$ during PDT. (A) CL imaging of tumor bearing mice after intratumor injection of DCM-Cl-OH and DCM-Cy with or without RB after 1 min irradiation. (B) Quantification of the chemiluminescence intensity at the same condition. Error bars represent standard deviations ($n = 3$).

plied to cellular, bacterial, and even *in vivo* models, providing precise sensing information of $^1O_2$ for the visualization of PDT treatment.

In summary, we have successfully developed an ultra-high signal-to-ratio near-infrared chemiluminescent probe DCM-Cy for high contrast monitoring $^1O_2$ during photodynamic therapy. By removing the methoxy unit to reduce the electron cloud density of the enolether unit, these CL probes can effectively suppress the self-photooxidation reaction, thereby minimizing the photoreaction induced background signals. Additionally, the substitution of the rigid and bulky adamantane units with a compact cyclobutane moiety significantly enhanced the cell permeability of the probe by approximately 6-fold. Consequently, DCM-Cy enables highly sensitive detection of endogenous $^1O_2$ in both living cells and pathogenic bacteria. Specifically, DCM-Cy demonstrated 95-fold ultra-high signal-to-noise imaging of intratumor $^1O_2$ in living

mice. Indeed, our "step-by-step" strategy addressed the limitations of traditional CL probes for $^1O_2$ determination and improving their biological applicability. We anticipate this straightforward design strategy will provide new insight into detecting of *in vivo* $^1O_2$ and pave the way for high-performance chemiluminescent probes.

Declaration of competing interest

The authors declare that they have no known competing financial interests or personal relationships that could have appeared to influence the work reported in this paper.

CRediT authorship contribution statement

Meiling Zhao: Writing – original draft, Software, Investigation, Formal analysis, Data curation, Conceptualization. **Yao Lu:** Validation, Formal analysis, Data curation, Conceptualization. **Yutao Zhang:** Writing – review & editing, Writing – original draft, Resources, Project administration, Methodology, Investigation, Funding acquisition, Formal analysis, Data curation, Conceptualization. **Haoyun Xue:** Validation, Methodology, Investigation. **Zhiqian Guo:** Writing – review & editing, Visualization, Validation, Supervision, Software, Resources, Project administration, Methodology, Investigation, Funding acquisition, Formal analysis, Data curation, Conceptualization.

Acknowledgments

This work was supported by National Natural Science Foundation of China (Nos. 32121005, 22225805, 22308101, and 32394001), Shanghai Science and Technology Innovation Action Plan (No. 23J21901600), Innovation Program of Shanghai Municipal Education Commission, Shanghai Frontier Science Research Base of Optogenetic Techniques for Cell Metabolism (Shanghai Municipal Education Commission, No. 2021 Sci & Tech 03–28), the China Postdoctoral Science Foundation (No. 2021M701199), Natural Science Foundation of Shanghai (No. 23ZR1416600).

Supplementary materials

Supplementary material associated with this article can be found, in the online version, at doi:10.1016/j.cclet.2024.110105.

References

[1] M. Garcia-Diaz, Y.Y. Huang, M.R. Hamblin, Methods 109 (2016) 158–166.
[2] Y. Wang, Y. Lin, S. He, et al., J. Hazard. Mater. 461 (2024) 132538.
[3] Z.Y. Jin, H. Fatima, Y. Zhang, et al., Adv. Ther. 5 (2022) 2100176.
[4] H. Kim, M. Yang, N. Kwon, et al., Bull. Korean Chem. Soc. 44 (2023) 236–255.
[5] X. Li, J.F. Lovell, J. Yoon, et al., Nat. Rev. Clin. Oncol. 17 (2020) 657–674.
[6] J.L. Wang, Y. Chen, J.X. Song, et al., Adv. Funct. Mater. 34 (2024) 2312162.
[7] G.Q. Jin, C.V. Chau, J.F. Arambula, et al., Chem. Soc. Rev. 51 (2022) 6177–6209.
[8] H. Wei, X. Li, F. Huang, et al., Chin. Chem. Lett. 34 (2023) 108564.
[9] E. Kozma, M. Bojtár, P. Kele, Angew. Chem. Int. Ed. 62 (2023) e202303198.
[10] Y. Jiang, Z. Zeng, J. Yao, et al., Chin. Chem. Lett. 34 (2023) 107966.
[11] S. Hackbarth, W. Islam, J. Fang, et al., Photochem. Photobiol. Sci. 18 (2019) 1304–1314.
[12] H. Wang, Z. Wang, Y. Li, et al., Small 15 (2019) 1902185.
[13] A. Looft, M. Pfitzner, A. Preuß, et al., Photodiagn. Photodyn. Ther. 23 (2018) 325–330.
[14] K. Murotomi, A. Umeno, M. Shichiri, et al., Int. J. Mol. Sci. 24 (2023) 2739.
[15] F. Zou, W. Zhou, W. Guan, et al., Anal. Chem. 88 (2016) 9707–9713.
[16] Y. Lang, S. Wu, Q. Yang, et al., Anal. Chem. 93 (2021) 9737–9743.
[17] S. Pfitzner, J.C. Schlothauer, B. Röder, et al., Laser Phys. 28 (2018) 085702.
[18] J.T. Ping, J.L. Qin, C. Zhou, et al., ChemNanoMat 6 (2020) 173-173.
[19] A. Prasad, M. Sedlářová, P. Pospíšil, Sci. Rep. 8 (2018) 13685.
[20] T. Entradas, S. Waldron, M. Volk, J. Photochem. Photobiol. B 204 (2020) 111787.
[21] H. Shen, F. Sun, X. Zhu, et al., J. Am. Chem. Soc 144 (2022) 15391–15402.
[22] C. Chen, H. Gao, H. Ou, et al., J. Am. Chem. Soc 144 (2022) 3429–3441.
[23] X. Duan, G.Q. Zhang, S. Ji, et al., Angew. Chem. Int. Ed. 61 (2022) e202116174.
[24] Q. Xiao, C. Xu, TrAC, Trends Anal. Chem. 124 (2020) 115780.
[25] O. Green, T. Eilon, N. Hananya, et al., ACS Cent. Sci. 3 (2017) 349–358.
[26] S. Joseph, S.K. Ashok Kumar, Coord. Chem. Rev. 496 (2023) 215408.
[27] Y. Zhang, C. Yan, C. Wang, et al., Angew. Chem. Int. Ed. 59 (2020) 9059–9066.
[28] R. Blau, O. Shelef, D. Shabat, et al., Nat. Rev. Bioeng. 1 (2023) 648–664.
[29] M. Yang, J. Huang, J. Fan, et al., Chem. Soc. Rev. 49 (2020) 6800–6815.
[30] N. Hananya, O. Green, R. Blau, et al., Angew. Chem. Int. Ed. 56 (2017) 11793–11796.
[31] J.C. Peterson, E. Arrieta, M. Ruggeri, et al., Biomed. Opt. Express 12 (2021) 272–287.
[32] Y. Wen, Z. Long, F. Huo, et al., Org. Chem. Front. 8 (2021) 1302–1314.
[33] M. Fadel, D.A. Fadeel, A. Tawfik, et al., J. Drug Deliv. Sci. Technol. 69 (2022) 103095.
[34] K.C. Yan, A.C. Sedgwick, Y. Zang, et al., Small Methods 3 (2019) 1900013.
[35] M. Yang, J. Zhang, D. Shabat, et al., ACS Sens. 5 (2020) 3158–3164.
[36] P.A. Rose, J.J. Krich, J. Phys. Chem. Lett. 14 (2023) 10849–10855.
[37] M.E. Roth-Konforti, C.R. Bauer, D. Shabat, Angew. Chem. Int. Ed. 56 (2017) 15633–15638.
[38] X. He, S. Koo, E. Obeng, et al., Coord. Chem. Rev. 492 (2023) 215275.
[39] M. Hirose, Y. Yoshida, K. Horii, et al., Arch. Oral Biol. 122 (2021) 105024.
[40] S. Sabbahi, L. Ben Ayed, M. Jemli, Appl. Water Sci. 8 (2018) 56.
[41] F. Hu, G. Qi, Kenry, et al., Angew. Chem. Int. Ed. 59 (2020) 9288–9292.
[42] Q. Jia, Q. Song, P. Li, et al., Adv. Healthc. Mater. 8 (2019) 1900608.
[43] Q. Zhao, G. Qing, J. Yu, et al., Chin. Chem. Lett. 35 (2024) 108535.